Holographic complexity of local quench at finite temperature

Dmitry S. Ageev*

Department of Mathematical Methods for Quantum Technologies, Steklov Mathematical Institute of Russian Academy of Sciences, Gubkin street 8, 119991 Moscow, Russia

(Received 16 October 2019; published 3 December 2019)

This paper is devoted to the study of the evolution of holographic complexity after a local perturbation of the system at finite temperature. We calculate the complexity using both the complexity = action (CA) and the complexity = volume (CV) conjectures. The CV calculation is performed in the small backreaction approximation and the CA one in the probe particle approximation. We find that the CV complexity of the total state shows the unbounded late-time linear growth. The CA computation shows linear growth with fast saturation to a constant value. We estimate the CV and CA complexity linear growth coefficients and show that finite temperature leads to violation of the Lloyd's bound for CA complexity. Also, it is shown that for the composite subsystem after the local quench, the state with minimal entanglement may correspond to the maximal complexity.

DOI: 10.1103/PhysRevD.100.126005

I. INTRODUCTION

The recent progress in understanding the relation between the gravitational degrees of freedom and quantum phenomena in the AdS/CFT correspondence includes holographic entanglement entropy [1–3], scrambling, the black hole information paradox, and quantum chaos [4–7]. Recently the notion of the quantum complexity of the state and holographic complexity have attracted considerable attention. There are different holographic proposals and conjectures concerning the quantum complexity [8–15]. The CV ("complexity = volume") conjecture relates complexity of a state to volume of a hypersurface in the bulk in the constant time slice. The CA ("complexity = action") conjecture states that the complexity is equal to the on-shell gravitational action evaluated in some special region of the bulk. Also, there are different covariant generalizations of these two proposals [4–15]. There are different setups where these proposals have been investigated. The first setup that has been considered is the thermofield double-state evolution in [4], with generalizations in [9,10,16–23]. Different complexity and entanglement proposals have been investigated for the state evolving after the global perturbation [23–29].

The process when the system evolves after the local perturbation is called the local quench. The 2d CFT admits a well-defined description of the local quenches [30]. The local quench has a well-defined gravity dual [31]. Different generalizations of this setup have been investigated further in [32–39]. In [40,41] we have investigated different versions of the holographic complexity proposals in the system following the local perturbation. We have considered the AdS_3 Poincare patch deformed by the static particle [31] as the background dual to the local quench. We have shown that the CV and CA prescriptions for a subsystems lead to a qualitatively different behavior, and we compared these prescriptions to the evolution of the entanglement entropy. The entanglement and the complexity show quite similar qualitative behavior in this process. Also, we have shown that the CA complexity for a local perturbation saturates Lloyd's bound on the complexification rate at the initial time moment.

This paper extends this study of the volume and the action complexity proposals to the case of the 2d CFT states at finite temperature evolving after the local perturbation. The holographic dual of this process is given by the one-sided planar BTZ black hole perturbed by the particle falling on the horizon [34]. The entanglement of the semi-infinite subsystem after the finite-temperature local quench does not show the late-time unbounded growth, in contrast to the $T = 0$ case. Instead of the late-time growth one can show that the entanglement saturates to some constant value [34]. We show that even after the time of the entanglement equilibration, the CV complexity shows unbounded linear growth. This is similar to the picture observed in the holographic description of

*ageev@mi-ras.ru

complexity in the thermofield double state: the complexity growth takes place even after the system is scrambled [8]. We estimate the linear growth coefficients for both CA and CV conjectures. The CA conjecture result (in the probe approximation) shows that at finite temperature, Lloyd's bound is violated for all values of temperature. Also, the straightforward estimation of the CA complexity does not lead to the unbounded linear late-time growth. The CV estimation shows that this bound is violated for some region of parameters of the system, like temperature T or perturbing operator dimension h. Note that the violation of Lloyd's bound has been observed and discussed in many works, including [16,18,19,22–24,42]. At the end of the paper we compare the evolution aspects of entanglement and the complexity of the composite system (two disjoint intervals). We find that the CV complexity estimation for such a system shows a (local) minimum of the entanglement at points where the complexity is maximal. In comparison to the $T = 0$ case the complexity grows much faster.

The paper is organized in the following way: In Sec. II, we describe the setup of the holographic local quench. Section III is devoted to the derivation of the entanglement entropy evolution of semi-infinite subsystem evolution. Sections IV and V are devoted to different approximations to the CA and the CV complexity and their computation. Finally Sec. VI is devoted to a discussion.

II. HOLOGRAPHIC DESCRIPTION OF CFT LOCAL QUENCH AT FINITE TEMPERATURE

The process in which the localized perturbation is excited at the initial time and then subsequently evolves is called the local quench. There are different protocols of local quench in the CFT. In this paper we restrict ourselves to the 2d CFT and assume that the quench is given by the insertion of the primary operator with the scaling dimension h at the point $x = 0$ and at time $t = 0$. The holographic dual of this quench is given by the particle of the fixed energy E deforming the background metric. This corresponds to the localized excitation carrying the same energy E in the CFT. In the case of 2d CFT one can obtain the analytical expression for the metric dual to the finite-temperature local quench [34]. Let us consider the one-sided planar BTZ black hole with the metric

$$ds^2 = \frac{L^2}{z^2}\left(-f(z)dt^2 + \frac{dz^2}{f(z)} + dx^2\right), \tag{1}$$

$$f(z) = 1 - Mz^2, \tag{2}$$

with temperature

$$T = \frac{1}{2\pi z_h}, \qquad M = 1/z_h^2. \tag{3}$$

The particle is falling on the black hole horizon $z = z_h$ following the trajectory $z = z(t)$ and deforming the vacuum metric (1). The deformed metric satisfies the equations of motion

$$R^{\mu\nu} - \frac{1}{2}g^{\mu\nu}R^{\mu\nu} + \Lambda g^{\mu\nu} = T^{\mu\nu}, \tag{4}$$

where $T^{\mu\nu}$ is the stress-energy tensor for the static particle

$$T^{\mu\nu} = \frac{8\pi m G_N}{\sqrt{-g}}\frac{\partial_t X^\mu \partial_t X^\nu}{\sqrt{-g_{\mu\nu}\cdot\partial_t X^\mu(t)\cdot\partial_t X^\nu(t)}}\delta(z - z(t))\delta^{d-1}(x_i), \tag{5}$$

and the explicit form of the particle trajectory is given by

$$z(t) = \frac{\beta}{2\pi}\sqrt{1 - \left(1 - \left(\frac{2\pi\varepsilon}{\beta}\right)^2\right)\left(1 - \tanh^2\left(\frac{2\pi}{\beta}t\right)\right)},$$
$$\beta = \frac{1}{T}. \tag{6}$$

Parameter ε is given by $z(0) = \varepsilon$, and in the dual language it corresponds to some "smearing" of the operator that perturbs the system. The particle action has the form

$$S = -mL\int\frac{1}{z}\sqrt{f(z) - \frac{\dot{z}^2}{f(z)}}dt, \tag{7}$$

where m is the mass of the particle and the dot denotes the derivative with respect to time t. The conformal dimension h of the corresponding quench operator in the dual CFT is given by the relation

$$h = \frac{mL}{2}, \tag{8}$$

and the particle has energy

$$E = mL\frac{\sqrt{1 - 4\pi^2T^2\varepsilon^2}}{\varepsilon}. \tag{9}$$

Instead of a straightforward solution of Eq. (4), it is convenient to use the following trick to obtain the explicit form of the dual metric. Consider the global AdS_3 deformed by the static particle

$$ds^2 = -d\tau^2(L^2 - \mu + R^2) + R^2d\phi^2 + \frac{L^2dR^2}{L^2 - \mu + R^2}, \tag{10}$$

where the particle rests at $R = 0$. Depending on parameter $\mu = 8GmL^2$, this space corresponds to the conical defect for $\mu < L^2$ and the BTZ black hole for $\mu > L^2$. One can relate the global AdS and the coordinates of the BTZ black hole (1) using the map from Appendix. A. Map (A1) relates

the static particle in the patch (10) at $R = 0$ and the trajectory (6) of the particle falling on the BTZ black hole horizon. Thus, applying coordinate transformation (A1), we obtain the full backreacted solution of (4). The solution is a time-dependent nondiagonal metric g of complicated form. The explicit form of this metric is

$$ds^2 = g_{ij}dx^i dx^j \tag{11}$$

where x_i corresponds to coordinates t and x. We do not write down metric g_{ij} explicitly in the text because it has a very complicated form. In what follows we also denote the dual metric as g. Now let us make some comments on the setup described here.

(i) The solution g describes the particle with the fixed energy falling on the one-sided planar black hole horizon and perturbing the geometry. For $T = 0$ the metric simplifies, and we write it down in Appendix B. This setup is described in [31] for $T = 0$ and in [34] for $T > 0$.[1]

(ii) The massive particle perturbing the eternal two-sided extension of the BTZ black hole is described in [33] as a holographic dual of the local operator quench of the thermofield double state.[2] The investigation of the complexity evolution in such perturbed states seems to be an interesting problem. However, in this paper we do not investigate full eternal black hole geometry, and we leave this to future research. In this sense our setup is closer to the studies of the dual of the one-sided black holes and their out-of-equilibrium physics; see [23,29] for examples of such complexity investigations.

(iii) Technically, in the calculations we are interested in the geometry under the black hole horizon $z < z_h$. We make comments on the CV and CA calculations in the next sections where it is appropriate to do so. It is worth noting that typically the Wheeler–de Witt (WdW) patch can probe behind the black hole horizon. Also, it is important for us to work in the BTZ-Schwarzschild patch where the massive particle's worldline is only part of the Kruskal patch worldline (see discussion in [33] and Fig. 2 in this work). The process of the particle falling, as well as a Penrose-like diagram, is presented in Fig. 2.

III. ENTANGLEMENT DYNAMICS AFTER LOCAL QUENCH

First we describe the entanglement entropy evolution in the system dual to the holographic setup described in Sec. II. The entanglement evolution in this model was described in [34]. According to the Hubeny-Rangamani-Takayanagi (HRT) formula the holographic entanglement entropy (HEE) of the interval $A \in (\ell_1, \ell_2)$ at time t is given by the geodesic $\gamma(x) = \gamma(x, \ell_1, \ell_2, t)$ anchored on the boundary at $x = \ell_1$ and $x = \ell_2$, i.e., satisfying $\gamma(\ell_1, \ell_1, \ell_2, t) = 0$ and $\gamma(\ell_2, \ell_1, \ell_2, t) = 0$. The HRT formula has the form

$$S_{\mathrm{HEE}}(\ell_1, \ell_2, t) = \frac{\mathcal{L}}{4G}, \tag{12}$$

where $\mathcal{L} = \mathcal{L}(\ell_1, \ell_2, t)$ is the (renormalized) length of the geodesic γ. In general, there are two ways to obtain $\mathcal{L}$. The first one is to compute the geodesic length in the background (10) and then, using (A1), map it to the planar BTZ patch (1). In this way one can get the exact answer for $\mathcal{L}(\ell_1, \ell_2, t)$ where ℓ_1, ℓ_2 and t are arbitrary; see [34] for a detailed study. Another way is to get a good approximation to $\mathcal{L}$ as follows. First one has to fix γ to that of the unperturbed background corresponding to $\mu = 0$; i.e., we fix $\gamma = \gamma_{\mathrm{BTZ}}$ where

$$\gamma_{\mathrm{BTZ}}(x, \ell_1, \ell_2) = \frac{2e^{\sqrt{M}(\ell_1+\ell_2)/2}}{\sqrt{M}} \frac{\sqrt{\sinh\left(\sqrt{M}(x-\ell_1)\right)\sinh\left(\sqrt{M}(\ell_2-x)\right)}}{e^{\sqrt{M}\ell_1} + e^{\sqrt{M}\ell_2}} \tag{13}$$

is the geodesic in the constant time slice of the BTZ black hole. Then we approximate the length $\mathcal{L}$ of this curve by the length of the curve given by parametrization (13) (unperturbed geodesic) embedded in the perturbed metric g. In other words, we compute $\mathcal{L}$ from the induced metric on the unperturbed geodesic in the deformed background with the metric g. In [31,37] it was shown that this procedure leads to very good qualitative (and for small M, quantitative) agreement with the exact answer, and when μ is small, this agreement becomes quantitative.

In Fig. 1 we present the evolution of the entanglement entropy of the semi-infinite subsystem $x > 0$. In contrast to the case $T = 0$ (where the entanglement shows the unbounded logarithmic growth), for $T > 0$ the entanglement entropy saturates to a constant value after some time. This is in agreement with the evolution picture obtained in [34]. Let us briefly summarize this section as follows:

(i) The behaviors of the entanglement entropy difference ΔS for an infinite subsystem for $T = 0$ and for $T > 0$ are different. For zero temperature ΔS shows an unbounded growth, and for $T > 0$ it saturates at late times. It is assumed that ΔS is the excitation of the entanglement over the equilibrium value corresponding to some thermal state with fixed T.

(ii) One can use "stationary geodesic approximation" as in [31] to get a good approximation capturing all

[1]Note that the explicit form of the metric is not written in these works.

[2]There are indications that planar one-sided black holes are dual to the special states called "thermal pure states"; see for example the discussions in [43].

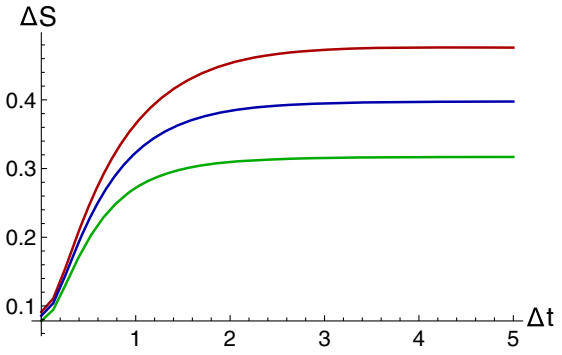

FIG. 1. The evolution of the entanglement entropy for the semi-infinite system $x > 0$. In this plot $\mu = 0.1$, $\varepsilon = 0.25$. Curves of different colors correspond to $M = 0.5,\ 1,\ 2$ from top to bottom, respectively. Here ΔS denotes the excitation of the entanglement above the equilibrium thermal state with a fixed $M = 0.5,\ 1,\ 2$ respectively.

the main features of the entanglement behavior for small μ. In [31] it was shown that for small μ the difference between the exact answer and that obtained in this approximation is negligible.[3] For $T > 0$ we see that the qualitative picture is also the same as for the exact answer from [34].

IV. ACTION COMPLEXITY

Consider now how the CA conjecture works in our setup. The particle backreaction leads to the complicated deformation of the WdW patch. The calculation of the action in such deformed regions is too complicated. We are not going to proceed in this way, and we restrict ourselves to the much simpler case when the backreaction of the particle is negligible. Of course, this approximation may miss some important aspects of the complexity evolution. On the other hand, it admits the analytical treatment and can still give us some insights and intuition related to the complexity evolution after the local quench. The model of the probe particle falling on the black hole in the probe approximation still serves as a nontrivial model to study. It is dual to the precursor perturbation with growing operator size evolving in a quantum system at finite temperature. For example, in [5,6] this simple model involving the probe particle has been used to investigate the dynamics of the operator size growth. In [44,45] a similar setup for the CA complexity and probe approximation for the string in AdS has been considered.

This implies that the action of our system consists of the gravity action on the static background and the particle action. Following the CA prescription, the complexity of the state at time τ is proportional to the on-shell gravitational and matter action restricted to the special region bounded by null rays emanating from the boundary

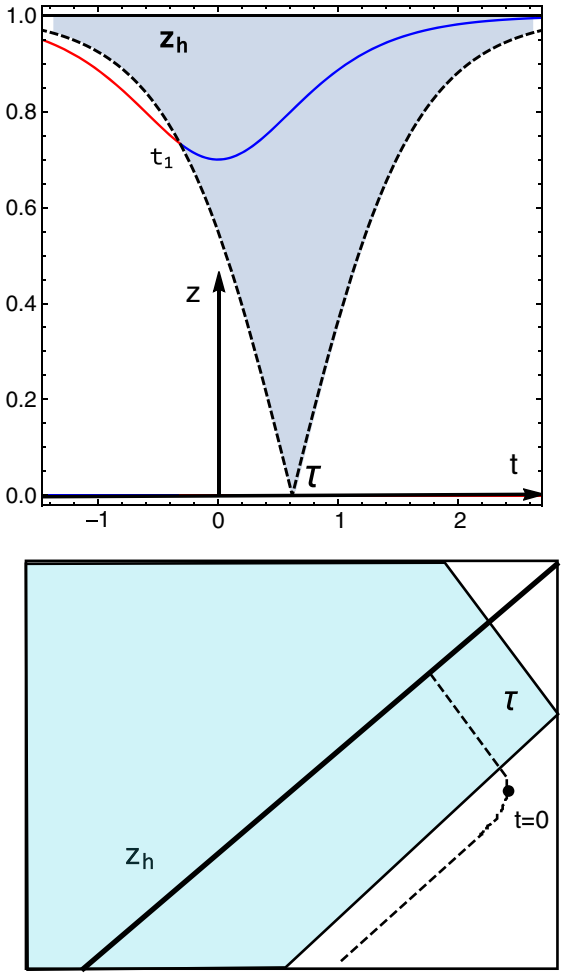

FIG. 2. Penroselike diagram of the right picture. The dashed line is the massive particle worldline. The cyan shaded region is the WdW plot at time moment τ. The black dot corresponds to the "quench time" $t = 0$.

at time τ. This region is called the WdW patch, and the action I_{WdW} in this patch is related to the complexity as

$$\mathcal{C}_{\mathrm{CA}} = \frac{I_{\mathrm{WdW}}}{\pi} = \frac{1}{\pi}(I_{\mathrm{gravity}} + I_{\mathrm{particle}}). \tag{14}$$

The complexity of formation (with respect to the static unperturbed BTZ black hole) in the probe particle approximation reduces to the particle action as[4]

$$\Delta\mathcal{C}_{\mathrm{CA}} = \frac{1}{\pi}(I_{\mathrm{gravity}} + I_{\mathrm{particle}}) - \frac{1}{\pi}I_{\mathrm{gravity}} = \frac{1}{\pi}I_{\mathrm{particle}} \tag{15}$$

because the particle is not backreacting. Thus, in the probe approximation the time-dependent part of the formation complexity is the particle action swept by the WdW patch. The probe limit is easily generalized from the AdS_3 case to general dimensions. Null rays bounding the WdW

[3]Also, see further investigation in [37].

[4]Due to this simplification, we are not focusing on the physics behind the horizon.

patch corresponding to the state at boundary time τ have the form

$$z = \pm z_h \tanh\frac{t-\tau}{z_h}. \tag{16}$$

Massive particle action S between time moments t_1 and t_2 is given by

$$S = -mL\int_{t_1}^{t_2}\frac{2\bar{E}}{(\bar{E}^2 z_h^2+1)\cosh(\frac{2t}{z_h})-\bar{E}^2 z_h^2+1}dt, \tag{17}$$

$$\bar{E} = \frac{E}{mL}. \tag{18}$$

The intersection picture of the WdW patch and the particle worldline is presented in Fig. 2. Note that from Fig. 2, one can see that the complexity of the state depends on times $t<0$ (in Fig. 2, the blue part of the worldline curve extends to the region $t<0$). Note that the quench position is $\tau=0$ and $x=0$. This means that, according to the canonical CA prescription, the complexity of the state after the quench strongly depends on the preparation protocol of the state. Also, this could be the drawback of the particular holographic model of local quench. Note that this model has time-reversal symmetry (also see the discussion on a related issue in [40,41]). For $\tau>0$ time t_1 in the formula (17) is given by

$$t_1 = z_h\log\left(\sqrt{\frac{\left(2z_h\sqrt{(z_h^2-\varepsilon^2)\sinh^2(\frac{\tau}{z_h})}-\varepsilon^2\right)(\sinh(\frac{\tau}{z_h})+\cosh(\frac{\tau}{z_h}))}{(2z_h^2-\varepsilon^2)\sinh(\frac{\tau}{z_h})+\varepsilon^2\cosh(\frac{\tau}{z_h})}}\right), \tag{19}$$

$$\Delta\mathcal{C} = -\frac{mL}{\pi}\left(\operatorname{arccot}\left(\frac{2\pi T}{\bar{E}}\right)+\operatorname{arccot}\left(\frac{2\pi T\sinh(2\pi T\tau)}{\sqrt{\bar{E}^2+4\pi^2T^2}-\bar{E}\cosh(2\pi T\tau)}\right)\right), \tag{20}$$

and $t_2\to\infty$. The behavior of the CA complexity given by formula (20) is presented in Fig. 3. After integration the explicit formula for the complexity growth has the form

$$\Delta\mathcal{C}\approx -h\left(1+\frac{2h}{\pi}\operatorname{arccot}\left(\frac{4h\pi T}{E}\right)\right)+\frac{(E+\sqrt{E^2+16h^2\pi^2T^2})}{\pi}\tau. \tag{21}$$

For the limit $T\to 0$ we reproduce the result of [40,41] where the saturation of Lloyd's bound at the initial time moment $\tau\to 0$ after perturbation was found. The temperature $T>0$ correction to the complexification rate at $\tau\to 0$ has the form

$$\frac{d\Delta\mathcal{C}}{dt}\approx\frac{2E}{\pi}+\frac{8h^2\pi T^2}{E}. \tag{22}$$

From (22) we see that temperature corrections lead to the violation of Lloyd's bound for all values of temperature.[5] The complexity for subsystems has a qualitative behavior similar to the one observed in [40,41], so we do not analyze it here in detail.

[5]Typically, Lloyd's bound is considered for the complexity.

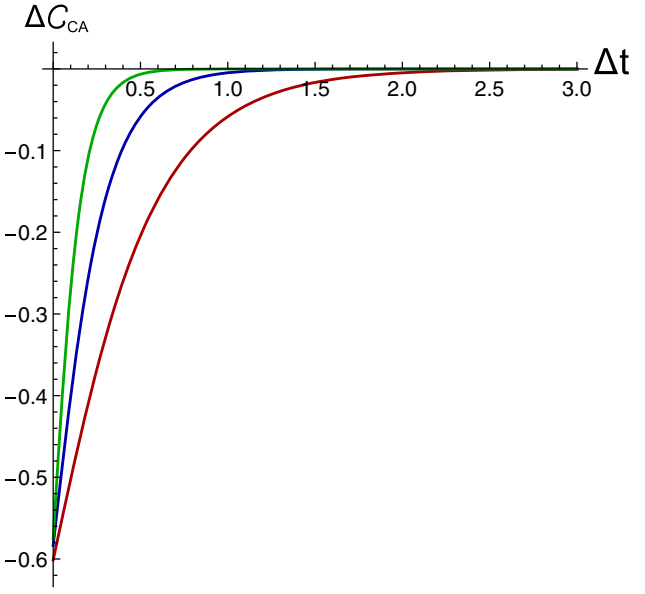

FIG. 3. The growth of the CA complexity after a local quench calculated in a probe approximation. The green curve corresponds to the temperature $T=1.5$, the blue one to $T=0.8$, and the red one to $T=0.6$. The energy of the particle $E=0.25$ is fixed. In this plot we assume that the complexity is normalized, i.e., $\Delta\mathcal{C}_{\mathrm{CA}}=\Delta\mathcal{C}_{\mathrm{CA}}/(mL)$. Expanding this expression at $\tau\to 0$ in (21), we find that the complexity exhibits the linear growth of the form where we used $m=2h/L$.

V. VOLUME COMPLEXITY

To calculate the CV complexity for the stationary dual background, one has to find the volume enclosed by the minimal hypersurface spanned on the boundary at time τ. There are different versions of covariant generalizations of the CV complexity proposal. In this paper we use an approximation similar to the one described in Sec. III for the entanglement entropy. As we mentioned at the end of Sec. III, it was shown to be a good approximation for entanglement; thus, we expect that it will also capture the evolution of the CV complexity correctly. Also, one can check that for $T = 0$ the analytical regimes from [40] for complexity are in agreement with this approximation. Following this approximation we choose the HRT surface for the subsystem to be that of the BTZ black hole with fixed T. This HRT surface is the geodesic configuration in the fixed constant time slice τ. Next, according to the CV prescription for subregions, we integrate the volume of constant time slice restricted by this HRT. Namely, we approximate the volume complexity as

$$\mathcal{C}_{\mathrm{CV}} \approx \frac{\mathcal{V}}{GL}, \tag{23}$$

where $\mathcal{V}$ is the volume of the constant time slice of the background with the metric g at the fixed time τ,

$$\mathcal{V} = \iint (\sqrt{\det \Sigma_\tau} - \sqrt{\det \Sigma_\tau}|_{\mu=0}) dx dz. \tag{24}$$

Here Σ_τ is the constant time slice volume form, and the second term corresponds to the constant time slice volume of the BTZ black hole ($\mu = 0$).[6]

To get some qualitative understanding of the gravitational dynamics of this model, we present a plot of the renormalized Σ_τ in Fig. 4. We see that at the initial time moment $\tau = 0$, gravitational perturbation starts from the boundary $z = 0$. Then the perturbation propagates to the horizon. Near the horizon at some time, it splits into two parts consisting of two large tails touching the boundary approximately at $\tau = x$. Each tail becomes more dense closer to the horizon. In the near-horizon zone they form a very dense gravitational perturbation. The whole late-time structure looks like a "wormhole" connecting the position of two "quasiparticles" in the boundary theory.

Now let us turn to the description of the complexity growth of the total state using formula (23). Calculating the integral in (24) numerically, we get the time dependence with fixed ε, μ and M. We present the result of the calculation in Fig. 5. We see that at the initial stage $\tau \to 0$, we get the quadratic growth. This is the common

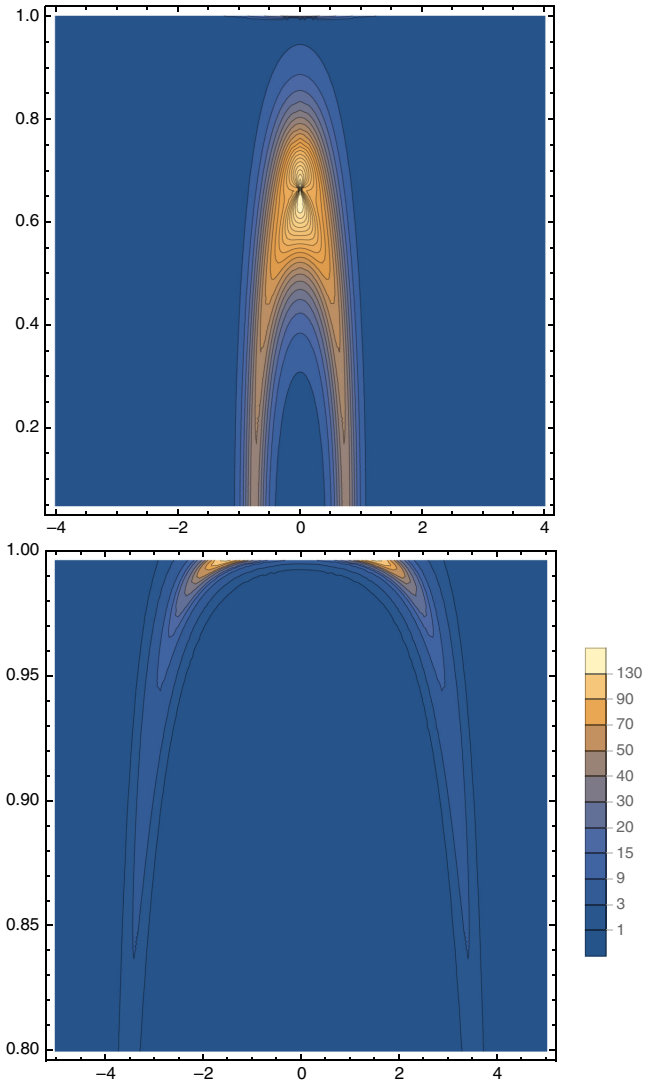

FIG. 4. The density of the (renormalized) volume Σ with $\mu = 0.1$, $M = 1$, $\varepsilon = 0.25$. The left plot corresponds to $\tau = 0.75$ and the right one to $\tau = 4$.

point when the dual description involves geometric quantities like the hypersurfaces stretched from the boundary [46]. After the quadratic growth we have the regime of linear unbounded growth of the complexity $\Delta\mathcal{C}$. In the case of $T = 0$ we see that this growth is not linear. The late-time linear growth is the consequence of the fast unbounded growth of the gravitational perturbation that spreads over the black hole background.

Let us outline now how this is reflected in the behavior of the subsystem CV complexity. First let us consider the single interval as the subsystem. The evolution is similar to the total system case except for times $t \approx \ell$, where one can observe a sharp decay of complexity to the equilibrium values. When $\ell \to \infty$, the time when decay starts shifts as $t \to \infty$, and we get an infinite linear growth. By naive dimensional analysis one can estimate this universal linear growth (of volume) as

[6]Note that this quantity is also called the complexity of formation. Here we refer to it as just complexity.

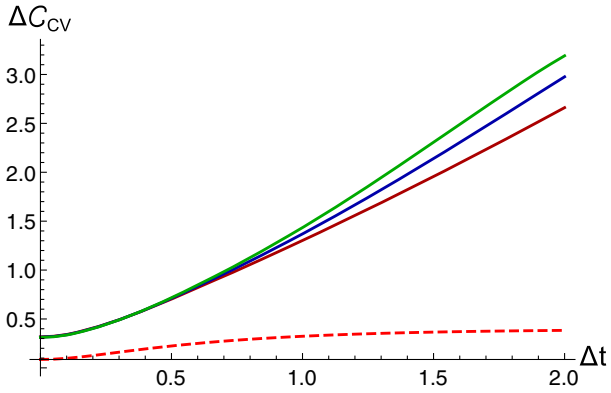

FIG. 5. The CV complexity evolution of the total system for different values of temperature. The different solid curves correspond to different colors: $M = 1$ (red curve), $M = 1.5$ (blue curve), and $M = 2$ (green curve) with the parameter values $\varepsilon = 0.25$ and $\mu = 0.1$. The dashed line corresponds to the entanglement evolution for the semi-infinite system $x > 0$ with $M = 1$. Note that here we plot the rescaled CV complexity, i.e., $\mathcal{C}_{\mathrm{CV}} \to \mathcal{C}_{\mathrm{CV}} \cdot GL$.

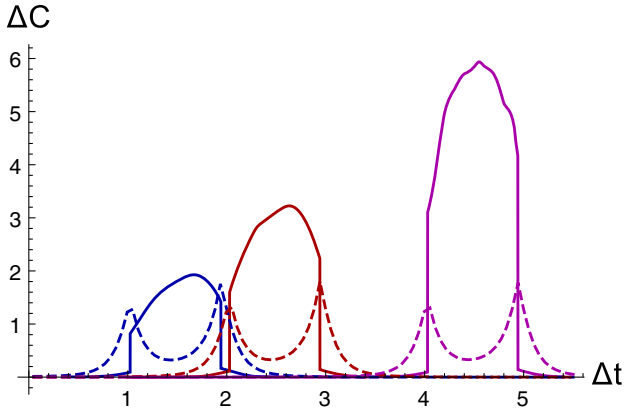

FIG. 6. The CV complexity evolution (solid curves) and the entanglement entropy (dashed curve) for two disjoint interval subsystems. The blue curves correspond to subsystem $x \in (-2, 1) \cup (1, 2)$, red curves to $x \in (-3, -2) \cup (2, 3)$, and the magenta ones to $x \in (-5, -4) \cup (4, 5)$. The entanglement entropy values are rescaled 20 times to compare with the complexity, and the complexity is rescaled as $\mathcal{C}_{\mathrm{CV}} \to \mathcal{C}_{\mathrm{CV}} \cdot GL$.

$$\Delta\mathcal{V} \sim \frac{\mu M}{\varepsilon} \cdot t, \tag{25}$$

and the numerical calculations with small ε and μ show that this relation takes place. Using this result we get the linear growth of complexity in the form

$$\Delta\mathcal{C} \sim 32\pi^2 T^2 \sqrt{E^2 + \pi^2 h^2 T^2} \cdot t \tag{26}$$

which violates Lloyd's bound for some values of T and h.

Now let us consider the complexity evolution for two disjoint intervals. In this case the comparison of the complexity of this subsystem with the entanglement evolution shows the difference between these two quantities. For simplicity we take two intervals of the length ℓ separated by the distance d located symmetrically with respect to the quench point $x = 0$. We present the evolution of entanglement and complexity for this system in Fig. 6. The entanglement evolution shows two sharp peaks approximately at times $\tau_1 = d/2$ and $\tau_2 = d/2 + \ell$. Between these two times the entanglement has a minimum approximately at $\tau_3 = d/2 + \ell/2$. There are two sets of competing HRT surfaces connecting intervals—the "disjoint" set corresponding to the geodesics spanned on the interval on each side of the quench separately and the "connected" set corresponding to the geodesics spanned on the endpoints of different intervals. In the early and late (before the first peak and after the last peak in the entanglement) stages of evolution, the disconnected set dominates. This leads to the slow growth and decay of complexity at these stages. However, in the intermediate regime between τ_1 and τ_2, the complexity exhibits a discontinuous jump, followed by fast saturation to the maximum and rapid decay at a time approximately corresponding to the entanglement minimum. For increasing $d \to \infty$ the maximal value of complexity grows. This is in contrast to the case of $T = 0$ where this growth is very slow for large d.

VI. DISCUSSION AND SUMMARY

This paper is devoted to the study of the holographic complexity of the finite-temperature state in two-dimensional conformal field theory that evolves after the perturbation by a local precursor. This precursor is the primary operator with the scaling dimension h. From the holographic viewpoint this process is described by the point particle falling on the horizon of a one-sided planar BTZ black hole. The exact metric for this process is known explicitly. We calculate the CA and the CV complexity evolution in this holographic background. We make the approximate calculation for both CA and CV prescriptions. One should note that in the CA computation, we focused on the matter contribution, while in the CV the main effects are produced from gravitational perturbations. In principle, the gravitational contribution can become comparable to the matter one in the CA computation even in the $\mu \to 0$ limit. In this sense the comparison between the CA and the CV complexities in the approximations we made is not really an apples-to-apples comparison. However, it gives some insight into these complexities separately. We leave the derivation of the exact answer for the gravitational contribution in the CA complexity, as well as the consideration of the perturbed thermofield or "eternal black hole + particle" system, for future research. For the CA proposal we restrict ourselves to the case of a probe particle approximation. We find the explicit formula describing the evolution of the action complexity. The CA evolution consists of the linear growth stage and the saturation at late times.

Instead of the saturation one can expect here the unbounded linear growth, as different works predict [7,8]. To get the late-time linear growth, one has to incorporate additional assumptions. There are different examples existing in the literature where one has to involve additional considerations to get the desired linear growth of the system. These examples are different dual models of the one-dimensional strongly coupled systems [47]. Reference [47] introduces the special boundary terms in the action, and Ref. [48] uses the finite bulk cutoff to get linear growth. It would be interesting to investigate the modification of our setup to get the linear late-time growth. Also, our calculation is performed in the approximate regime. So taking into account the gravitational backreaction effects may change the situation and produce the desired linear growth behavior from first principles.

As in the thermofield state the CV conjecture calculation demonstrates the late-time unbounded linear growth without any additional considerations. However, in contrast to the CA conjecture, the CV complexity shows the initial quadratic growth usually corresponding to the equilibration of the local correlations in the system. We give the simple estimate of the linear growth coefficient and find that it violates Lloyd's bound for some temperature values. After the quench gravitational perturbation moves towards black hole horizon position. Next, the perturbation splits into two localized "tubes" connected through the near-horizon region. Of course this calculation is performed in the constant time slice approximation, so there is a question of the regime of validity of this approximation. The picture shown here also supports the idea that the gravitational contribution may change the CA evolution in the desired way. Finally, we compare the entanglement and complexity evolution for a system of disjoint intervals and find that the (local) minimum of the entanglement is realized when the complexity is maximal. This raises the question of the relation between complexity and the quasiparticle picture. Remember that the entanglement is in good correspondence with this picture.

The evolution of the holographic complexity following the quenches of different types has been considered in different works [23–25,27–29]. These investigations are typically concerned with the global quenches described by the Vaidya geometry in which a thin shell collapses into one-sided [23–25,27–29] or two-sided black holes [27]. In this sense our work is analogous to the one-sided setup. As in our local quench, the CV complexity for the total state in one-sided collapse shows the late-time linear growth. The subregion CV duality also shows similarities with the global quench setup from [28]. The violation of Lloyd's bound has been observed in our case both for the CV and CA pictures and also takes place in some works on global quenches; see for example [16,18,19,22–24,42]. It is also interesting to compare this with different complexity results concerning nonequilibrium states developed in [49–54].

ACKNOWLEDGMENTS

I would like to thank I. Ya. Aref'eva for comments on the early version of this text and Shira Chapman for discussions. This work is supported by the Russian Science Foundation (Project No. 17-71-20154).

APPENDIX A: RELATION BETWEEN GLOBAL AND POINCARE CHARTS

Formula (A1) is the mapping of the metric (10) with $\mu = 0$ (global AdS) to the BTZ black hole (1) with fixed mass M. To map the geodesic $R = 0$ in the global coordinate to the particle falling in the bulk starting from the point $z = \varepsilon$, one must use the formula

$$\begin{aligned}
\phi &= \arctan\left(\frac{\varepsilon\sqrt{M}\sinh(\sqrt{M}x)}{\sqrt{1-Mz^2}\cosh(\sqrt{M}t)-\sqrt{1-\varepsilon^2M}\cosh(\sqrt{M}x)}\right),\\
\tau &= -\arctan\left(\frac{\varepsilon\sqrt{M}\sqrt{1-Mz^2}\sinh(\sqrt{M}t)}{\sqrt{1-\varepsilon^2M}\sqrt{1-Mz^2}\cosh(\sqrt{M}t)-\cosh(\sqrt{M}x)}\right),\\
R &= \frac{L}{2\varepsilon Mz}\sqrt{\mathcal{A}_1+\mathcal{A}_2},\\
\mathcal{A}_1 &= -8\sqrt{1-\varepsilon^2M}\sqrt{1-Mz^2}\cosh(\sqrt{M}t)\cosh(\sqrt{M}x)-4\varepsilon^2M+3-Mz^2,\\
\mathcal{A}_2 &= (2-2Mz^2)\cosh^2(\sqrt{M}t)+(1-Mz^2)\cosh(2\sqrt{M}t)+2\cosh(2\sqrt{M}x).
\end{aligned} \tag{A1}$$

APPENDIX B: EXPLICIT FORM OF THE METRIC

In this appendix, we derive the explicit form of the metric dual to the local holographic quench. The explicit form of the metric (of reasonable size) can be obtained only for $M = 0$. The global AdS_3 metric deformed by a static point particle of mass m is given by

$$ds^2 = -d\tau^2(L^2-\mu+R^2)+R^2d\phi^2+\frac{L^2dR^2}{L^2-\mu+R^2}, \tag{B1}$$

where $\mu = 8mGL^2$. For simplicity we take $L = 1$.

Then, we obtain the holographic dual of the local quench by applying to (B1) the following coordinate transformation:

$$\phi = \arctan\left(\frac{2\alpha x}{\alpha^2+t^2-x^2-z^2}\right), \tag{B2}$$

$$\tau = \arctan\left(\frac{2\alpha t}{\alpha^2-t^2+x^2+z^2}\right), \tag{B3}$$

$$R = \frac{\sqrt{\alpha^4+2\alpha^2,(t^2+x^2-z^2)+(-t^2+x^2+z^2)^2}}{2\alpha z}, \tag{B4}$$

which is the $T = 0$ limit of (A1). After some algebra we get the metric in the form

$$\begin{aligned} ds^2 = &\frac{1}{z^2}\frac{(\alpha^2dx-2txdt+dx(u-z^2)+2xzdz)^2}{\alpha^4+2\alpha^2(u-z^2)+(z^2-v)^2} \\ &-\frac{1}{z^2}\frac{(\alpha^4+2\alpha^2(u+z^2(1-2\mu))+(z^2-v)^2)(\alpha^2dt+(u+z^2)dt-2t(xdx+zdz))^2}{(\alpha^4+2\alpha^2(u+z^2)+(z^2-v)^2)^2} \\ &\times\frac{1}{z^2}\frac{(\alpha^4dz+2\alpha^2(udz-z(tdt+xdx))+(v-z^2)(-2tzdt+2xzdx+(v+z^2)dz))^2}{(\alpha^4+2\alpha^2(u-z^2)+(z^2-v)^2)(\alpha^4+2\alpha^2(-2\mu z^2+u+z^2)+(z^2-v)^2)}, \end{aligned} \tag{B5}$$

where we introduced $u = t^2-x^2$ and $v = t^2+x^2$.

[1] S. Ryu and T. Takayanagi, Holographic Derivation of Entanglement Entropy from AdS/CFT, Phys. Rev. Lett. **96**, 181602 (2006).
[2] M. Van Raamsdonk, Building up spacetime with quantum entanglement, Gen. Relativ. Gravit. **42**, 2323 (2010); Int. J. Mod. Phys. D **19**, 2429 (2010).
[3] B. Swingle, Entanglement renormalization and holography, Phys. Rev. D **86**, 065007 (2012).
[4] L. Susskind, Computational complexity and black hole horizons, Fortschr. Phys. **64**, 24 (2016); **64**, 44(A) (2016).
[5] L. Susskind, Why do things fall?, arXiv:1802.01198.
[6] D. S. Ageev and I. Y. Aref'eva, When things stop falling, chaos is suppressed, J. High Energy Phys. 01 (2019) 100.
[7] L. Susskind, Three lectures on complexity and black holes, arXiv:1810.11563.
[8] D. Stanford and L. Susskind, Complexity and shock wave geometries, Phys. Rev. D **90**, 126007 (2014).
[9] A. R. Brown, D. A. Roberts, L. Susskind, B. Swingle, and Y. Zhao, Holographic Complexity Equals Bulk Action?, Phys. Rev. Lett. **116**, 191301 (2016).
[10] A. R. Brown, D. A. Roberts, L. Susskind, B. Swingle, and Y. Zhao, Complexity, action, and black holes, Phys. Rev. D **93**, 086006 (2016).
[11] M. Alishahiha, Holographic complexity, Phys. Rev. D **92**, 126009 (2015).
[12] P. Caputa, N. Kundu, M. Miyaji, T. Takayanagi, and K. Watanabe, Anti-de Sitter Space from Optimization of Path Integrals in Conformal Field Theories, Phys. Rev. Lett. **119**, 071602 (2017).
[13] P. Caputa, N. Kundu, M. Miyaji, T. Takayanagi, and K. Watanabe, Liouville action as path-integral complexity: From continuous tensor networks to AdS/CFT, J. High Energy Phys. 11 (2017) 097.
[14] T. Takayanagi, Holographic spacetimes as quantum circuits of path-integrations, J. High Energy Phys. 12 (2018) 048.
[15] R. Abt, J. Erdmenger, H. Hinrichsen, C. M. Melby-Thompson, R. Meyer, C. Northe, and I. A. Reyes, Topological complexity in $AdS_3/CFT2$, Fortschr. Phys. **66**, 1800034 (2018).
[16] D. Carmi, S. Chapman, H. Marrochio, R. C. Myers, and S. Sugishita, On the time dependence of holographic complexity, J. High Energy Phys. 11 (2017) 188.
[17] S. Chapman, H. Marrochio, and R. C. Myers, Complexity of Formation in Holography, J. High Energy Phys. 01 (2017) 062.
[18] B. Swingle and Y. Wang, Holographic complexity of Einstein-Maxwell-Dilaton gravity, J. High Energy Phys. 09 (2018) 106.
[19] W. Cottrell and M. Montero, Complexity is simple!, J. High Energy Phys. 02 (2018) 039.
[20] S. A. Hosseini Mansoori and M. M. Qaemmaqami, Complexity growth, butterfly velocity and black hole thermodynamics, arXiv:1711.09749.
[21] Y. Ling, Y. Liu, and C. Y. Zhang, Holographic subregion complexity in Einstein-Born-Infeld theory, Eur. Phys. J. C **79**, 194 (2019).
[22] Y. S. An and R. H. Peng, The effect of dilaton on the holographic complexity growth, Phys. Rev. D **97**, 066022 (2018).

[23] M. Alishahiha, A. Faraji Astaneh, M. R. Mohammadi Mozaffar, and A. Mollabashi, Complexity growth with Lifshitz scaling and hyperscaling violation, J. High Energy Phys. 07 (2018) 042.
[24] M. Moosa, Divergences in the rate of complexification, Phys. Rev. D **97**, 106016 (2018).
[25] M. Moosa, Evolution of complexity following a global quench, J. High Energy Phys. 03 (2018) 031.
[26] B. Chen, W. M. Li, R. Q. Yang, C. Y. Zhang, and S. J. Zhang, Holographic subregion complexity under a thermal quench, J. High Energy Phys. 07 (2018) 034.
[27] S. Chapman, H. Marrochio, and R. C. Myers, Holographic complexity in Vaidya spacetimes. Part II, J. High Energy Phys. 06 (2018) 114.
[28] Z. Y. Fan and M. Guo, Holographic complexity under a global quantum quench, arXiv:1811.01473.
[29] S. Chapman, H. Marrochio, and R. C. Myers, Holographic complexity in Vaidya spacetimes. Part I, J. High Energy Phys. 06 (2018) 046.
[30] P. Calabrese and J. Cardy, Entanglement and correlation functions following a local quench: A conformal field theory approach, J. Stat. Mech. (2007) P10004.
[31] M. Nozaki, T. Numasawa, and T. Takayanagi, Holographic local quenches and entanglement density, J. High Energy Phys. 05 (2013) 080.
[32] C. T. Asplund, A. Bernamonti, F. Galli, and T. Hartman, Holographic entanglement entropy from 2d CFT: Heavy states and local quenches, J. High Energy Phys. 02 (2015) 171.
[33] P. Caputa, J. Simon, A. Stikonas, T. Takayanagi, and K. Watanabe, Scrambling time from local perturbations of the eternal BTZ black hole, J. High Energy Phys. 08 (2015) 011.
[34] P. Caputa, J. Simon, A. Stikonas, and T. Takayanagi, Quantum entanglement of localized excited states at finite temperature, J. High Energy Phys. 01 (2015) 102.
[35] D. S. Ageev, I. Y. Aref'eva, and M. D. Tikhanovskaya, $(1+1)$-Correlators and moving massive defects, Teor. Mat. Fiz. **188**, 85 (2016) [Theor. Math. Phys. **188**, 1038 (2016)].
[36] D. S. Ageev and I. Y. Aref'eva, Holographic instant conformal symmetry breaking by colliding conical defects, Teor. Mat. Fiz. **189**, 389 (2016) [Theor. Math. Phys. **189**, 1742 (2016)].
[37] A. Jahn and T. Takayanagi, Holographic entanglement entropy of local quenches in AdS4/CFT3: a finite-element approach, J. Phys. A **51**, 015401 (2018).
[38] J. R. David, S. Khetrapal, and S. P. Kumar, Local quenches and quantum chaos from higher spin perturbations, J. High Energy Phys. 10 (2017) 156.
[39] T. De Jonckheere and J. Lindgren, Entanglement entropy in inhomogeneous quenches in AdS_3/CFT_2, Phys. Rev. D **98**, 106006 (2018).
[40] D. S. Ageev, I. Y. Aref'eva, A. A. Bagrov, and M. I. Katsnelson, Holographic local quench and effective complexity, J. High Energy Phys. 08 (2018) 071.
[41] D. Ageev, Holography, quantum complexity and quantum chaos in different models, EPJ Web Conf. **191**, 06006 (2018).
[42] A. Akhavan, M. Alishahiha, A. Naseh, and H. Zolfi, Complexity and behind the horizon cut off, J. High Energy Phys. 12 (2018) 090.
[43] A. Goel, H. T. Lam, G. J. Turiaci, and H. Verlinde, Expanding the Black Hole Interior: Partially Entangled Thermal States in SYK, J. High Energy Phys. 02 (2019) 156.
[44] K. Nagasaki, Complexity of AdS_5 black holes with a rotating string, Phys. Rev. D **96**, 126018 (2017).
[45] K. Nagasaki, Complexity growth of rotating black holes with a probe string, Phys. Rev. D **98**, 126014 (2018).
[46] H. Liu and S. J. Suh, Entanglement growth during thermalization in holographic systems, Phys. Rev. D **89**, 066012 (2014).
[47] A. R. Brown, H. Gharibyan, H. W. Lin, L. Susskind, L. Thorlacius, and Y. Zhao, The case of the missing gates: Complexity of Jackiw-Teitelboim gravity, Phys. Rev. D **99**, 046016 (2019).
[48] M. Alishahiha, On complexity of Jackiw-Teitelboim gravity, Eur. Phys. J. C **79**, 365 (2019).
[49] D. W. F. Alves and G. Camilo, Evolution of complexity following a quantum quench in free field theory, J. High Energy Phys. 06 (2018) 029.
[50] H. A. Camargo, P. Caputa, D. Das, M. P. Heller, and R. Jefferson, Complexity as a novel probe of quantum quenches: Universal scalings and purifications, Phys. Rev. Lett. **122**, 081601 (2019).
[51] S. Chapman, J. Eisert, L. Hackl, M. P. Heller, R. Jefferson, H. Marrochio, and R. C. Myers, Complexity and entanglement for thermofield double states, SciPost Phys. **6**, 034 (2019).
[52] T. Ali, A. Bhattacharyya, S. Shajidul Haque, E. H. Kim, and N. Moynihan, Time evolution of complexity: A critique of three methods, J. High Energy Phys. 04 (2019) 087.
[53] S. Banerjee, J. Erdmenger, and D. Sarkar, Connecting Fisher information to bulk entanglement in holography, J. High Energy Phys. 08 (2018) 001.
[54] T. Shimaji, T. Takayanagi, and Z. Wei, Holographic quantum circuits from splitting/joining local quenches, J. High Energy Phys. 03 (2019) 165.